Influence of H_2 adsorption on magnetic properties of Fe films on Cu(001)

R. Vollmer and J. Kirschner
Max-Planck-Institut für Mikrostrukturphysik, Weinberg 2, D-06120 Halle/Saale, Germany
(Received 20 July 1999)

It is shown that the tetragonally expanded fcc phase (phase I) of room-temperature-grown Fe films on Cu can be stabilized by hydrogen adsorption up to four monolayers (ML) while the uncovered Fe film starts to transform slightly above 3 ML to the fcc phase (phase II). The changes in the magnetic properties are closely related to the changes in the structure. The phase boundary between the fcc phase II and the bcc phase (phase III) is shifted by 2 ML to lower values upon hydrogen exposure of less than three langmuir after growth at $T \approx 300$ K. Growing the Fe films at 300 K under an H_2 atmosphere of $\approx 5 \times 10^{-8}$ mbar results in Fe films, where a spin reorientation transition at about 6 ML is observed. Starting at about 4–5 ML the Fe films transforms into the bcc phase. The structural and magnetic properties of these films are found to be very similar to those observed for low-temperature-grown (100 K) Fe films.

The puzzling structural and magnetic properties of fcc Fe films on Cu(001) have been investigated extensively in the past.[1–15] Fe films prepared by molecular-beam epitaxy at room temperature show a rich variety of structural and magnetic phases: At low Fe thickness below three to four monolayers (ML) the Fe film is tetragonally distorted (phase I or fct phase). The interlayer Fe distance is expanded by 5% to 1.87 Å.[7,8] At a thickness larger than about 4 ML the interlayer distance of the Fe film relaxes in its interior nearly to the value of ideal cubic symmetry (phase II). Only the interlayer distance of the first two layers remains expanded.[3] Parallel to the structural change the average magnetization of the Fe film drops to a value roughly equal to that of 2 ML Fe of phase I. Detailed experimental[16–21] and theoretical[22–26] investigations indeed revealed that the magnetic moment of the first and second layer couple ferromagnetically, while the deeper layers are antiferromagnetically aligned at temperatures lower than 200 K.[17] At a thickness of about 11 ML the fcc Fe film transforms into a bcc phase (phase III).[4,16,27] The easy axis of magnetization is perpendicular to the surface for phase I and II and switches in plane in the bcc phase III. The Fe film in phase I is reconstructed and shows a (4×1) superstructure for 2 ML thickness which change to a (5×1) superstructure for larger thickness.[7,8,32] In phase II a (2×1) reconstruction has been found at low temperatures.[3,31]

For Fe films grown at low temperatures (100 K) very different structural and magnetic properties have been reported.[19,20,28–30,33] The fct phase extends up to a thickness of about 5 ML.[33] Above that thickness the Fe film directly transforms into the bcc phase without going through the intermediate fcc phase II observed for the room-temperature-grown films. The investigation of the magnetic properties revealed that the magnetization of the low-temperature-grown Fe film is perpendicular to the surface for thicknesses below approximately 6 ML and it is parallel to the surface plane for thicker films.[30]

Despite the large interest the Fe/Cu(001) system received in the past, up to now little is known about the hydrogen adsorption on this surface. Hydrogen adsorbs dissociatively on the fcc Fe(001) surface.[32] The reconstructions in phase I persist upon hydrogen adsorption while for the reconstruction in phase II the authors of Ref. 32 observed a $p(2\times2)-p4g$ superstructure.

In the present study we use the intensity of low-energy electrons reflected from the sample vs beam energy measurements (IV-LEED) and the magneto-optical Kerr-effect (MOKE) to determine the structural and magnetic properties of *room-temperature*-grown fct/fcc Fe films on Cu(001) on hydrogen adsorption in the thickness range of the Fe between 0 and 13 ML. After the description of the experimental setup in Sec. I, we show in Sec. II A that the adsorption of H_2 switches the structure of a 4-ML-thick Fe film from fcc to fct, which is accompanied by the corresponding changes in the magnetic phases. This shift of the phase boundary between phase I and II is *reversible*, i.e., upon desorption of the hydrogen the film becomes unstable and switches back into the fcc structure. In Sec. II B it is shown that H_2 adsorption *irreversibly* shifts the thickness of the transition between phase II and III from about 10 ML down to 8 ML. Section II C presents the results obtained from room-temperature-grown Fe films with an H_2 atmosphere *during* the growth. In Sec. III we discuss our experimental results on the reversible hydrogen induced changes at the transition between phase I and phase II. The relevance of H_2 adsorption vs other properties like surface roughness for the magnetic behavior is discussed in view of the observed differences between low-temperature-grown Fe films and room-temperature-grown films reported in the literature. We conclude in Sec. IV that H_2 adsorption strongly affects the magnetic and structural properties of ultrathin Fe layers.

I. EXPERIMENT

Fe films of constant thickness as well as wedgelike samples were grown on a Cu(001) single crystal in a molecular-beam epitaxy apparatus (base pressure $<4\times10^{-11}$ mbar). In this investigation *all* films were grown at $T=293\pm1$ K. The flux of the Fe *e*-beam evaporator was calibrated by means of medium energy electron diffraction (MEED) prior to and after the growth of the wedges. The

thickness of the single Fe films were controlled directly by MEED. The growth rate was about 0.8 ML/min at a pressure of less than 4×10^{-10} mbar during evaporation. The absolute error in the thickness calibration of the single layers is about 0.2 ML. For the wedges the absolute error in the thickness at a certain position on the wedge is less than 0.2 ML plus 10% of the (nominal) thickness at that point. To remove the possibly adsorbed gas during the deposition of the film prior to the measurements the sample was annealed to 343 K for about 5 min. A standard static magneto-optical Kerr-effect (MOKE) setup has been used to measure the Kerr ellipticity at light wavelength of $\lambda=670$ nm.[34] For measurements in the polar Kerr geometry the angle between the incident light beam and the sample normal was about 6.5°. A dipole magnet was mounted at an angle of about 18.5° with respect to the sample normal parallel to the optical plane. For measurements in the longitudinal geometry the sample was rotated such that the angle between incident light beam and and sample normal was about 71.5°. In this geometry the axis of the magnet was nearly parallel to the surface of the sample. In all cases the Kerr ellipticity was measured. The maximum external field which could be reached at the sample was about 300 Oe. The $\langle 110\rangle$ azimuth of the Cu substrate was aligned parallel to the optical plane of the MOKE setup.

A standard LEED optics has been used for taking LEED images at (nearly) normal incidence of the electron beam. Measurements of the intensity of a specularly reflected *e* beam from the sample were performed at an angle of incidence of about 6° from normal and the intensity integrated over the spot was recorded as a function of the beam energy (IV-LEED).[35] Hydrogen exposure was performed by opening a leak valve and filling the chamber up to the desired pressure measured by a standard ionization gauge calibrated for N_2. No further adjustment or calibration was made. The true H_2 pressures may be a factor of approximately 3 larger.

II. RESULTS

A. Hydrogen adsorption on a 4-ML Fe film

Semiquantitative analysis of interlayer spacings by analysis of the energy dependence of a low-energy electron beam specularly reflected from a sample (IV-LEED) has been widely used in the identification of structural transition[15,36–40] in general and in the analysis of the structural transition at about 4 ML Fe on Cu(001) in particular.[12] It was found that the IV-LEED spectrum of the fcc Fe film looks very ''kinematical,'' i.e., has one relatively narrow peak close to each Bragg peak positions expected from a kinematic theory while for the fct structure a double peak structure is found around each kinematic energy peak position.[12] The splitting of the kinematical peak in this phase arises from the reconstruction of the film to a (5×1) superstructure, which introduces a vertical buckling of the Fe layers of the order of 0.1 – 0.3 Å.[7,8] However, the center of the double peak structure is shifted towards lower energies indicating an increased interlayer spacing of the Fe in phase I.

The intensity of the specularly scattered *e* beam from a 4-ML-thick Fe film on Cu(001) at $T=243$ K is shown in Fig. 1 for the nominally clean surface (solid line) and for the surface exposed to 2 langmuir (L) of H_2 (dashed line) in the energy range from 200 to 320 eV which is around the fifth-order kinematical peak position. The curve for the H-covered Fe films shows the typical double peak structure with maxima at about 239 and 273 eV. This double peak structure is known to be a signature of the tetragonally expanded phase I as mentioned above. The ''clean'' surface on the other hand has only a single peak at about 273 eV in this energy range and this is the signature of the fcc structure of phase II.

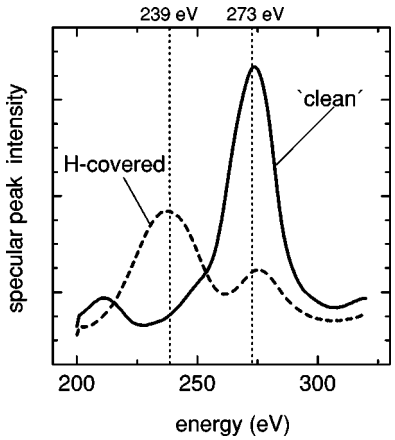

FIG. 1. Intensity of the specularly scattered *e* beam from a 4-ML-thick Fe film on Cu(001) as a function of the *e* beam energy for the ''clean'' and H-covered film. Peak positions at 239 and 273 eV are indicated by dotted lines.

The ratio of the IV-LEED intensity at 239 and 273 eV is plotted in Fig. 2(a) (top row panels) as a function of temperature. We observed no strong energy shift in the position of these two peaks during temperature cycling indicating a possible change in the amplitude of the buckling or the interlayer spacing. Therefore we take this ratio as a qualitative measure of the relative fraction of phase I and phase II. The film was exposed to 2 L H_2 at 243 K. After that IV-LEED curves were measured during a temperature cycle to 343 K and back to 243 K [Fig. 2(a)]. The low IV-LEED ratio on the branch for decreasing temperature indicates the complete disappearance of the peak at 239 eV in agreement with the findings of Refs. 12 and 41. Immediately after this measurement the hydrogen partial pressure was raised to 2×10^{-8} mbar and IV-LEED spectra were recorded. The resulting peak ratios are plotted in Fig. 2(b). The peak ratio is fully recovered after a hydrogen exposure of about 1 L. After that IV-LEED measurements during a complete temperature cycle to 343 K and back were recorded again. No significant difference between this second cycle displayed in Fig. 2(c) and the first one in Fig. 2(a) is observed.

For the investigation of the magnetic properties polar MOKE measurements were performed for the same sequence of temperature cycling and hydrogen adsorption. The result is plotted in Figs. 2(d)–(f). The open symbols represent the MOKE data at remanence while the data indicated with filled symbols were taken in an external field of about 250 Oe. While at low temperatures these data nearly coincide for the two kinds of measurements the remanence data drop earlier to zero, presumably because of domain formation near the Curie temperature as it was observed, for example, for thin Ni films on Cu(001).[42] This effect is observed for the hydrogen covered surface with increasing temperature and

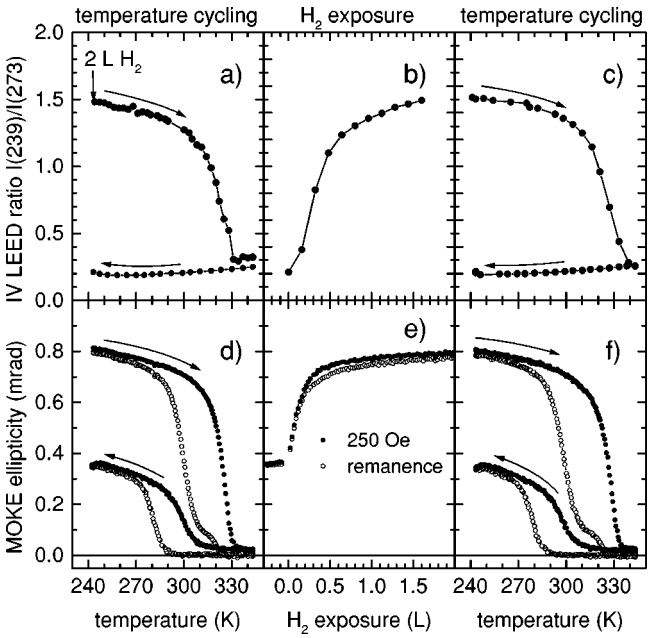

FIG. 2. IV-LEED ratio of the specularly reflected electron beam energy at 239 and 273 eV [panels (a)–(c)] and polar MOKE signal [panels (d)–(f)] from a 4-ML Fe/Cu(001) film. In (a) the IV-LEED ratio after exposure to 2 L H_2 is shown for the temperature increasing from 243 to 343 K and then back. Then at 243 K the hydrogen pressure is adjusted to 2×10^{-8} mbar. The resulting IV-LEED intensity ratio vs H_2 exposure is plotted in (b). Afterwards the temperature was cycled to 343 K and back again (c). (d)–(f) show the same sequence for the polar MOKE ellipticity. Solid symbols indicate measurements with an applied external field of about 250 Oe, open symbols the MOKE signal from the remanent magnetization.

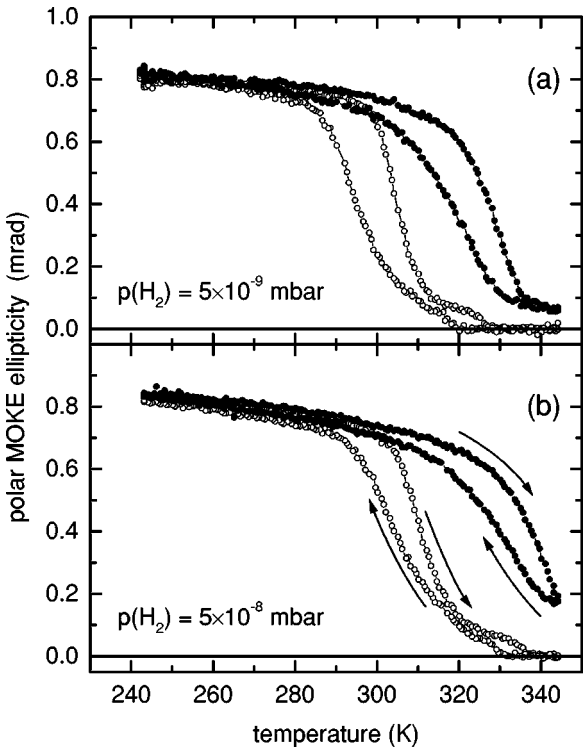

FIG. 3. Polar MOKE ellipticity of a 4-ML Fe film on Cu(001) vs sample temperature with an H_2 pressure of (a) 5×10^{-9} mbar and (b) 5×10^{-8} mbar. Open symbols indicate the remanent Kerr signal while solid symbols are the measurements with 250 Oe external field. The arrows in (b) on the curves indicate the direction of the temperature change.

on the way back to low temperatures. We focus now on the MOKE data taken with applied field (solid symbols in Fig. 2) where from the shape of the hysteresis curve we can assume a single domain state. There are two differences in the curves for decreasing and increasing temperature: (i) While the MOKE signal disappears on heating of the H-covered Fe film at about 330 K, the MOKE signal reappears upon cooling at a much lower temperature of 300 K, which is close to the observed Curie temperature of Fe films in phase II. (ii) After the temperature cycle from 243 to 343 K and back to 243 K the amplitude of the MOKE signal (even when extrapolated to 0 K) does not reach the level of the initial H_2 covered film. The signal is roughly halved and would correspond to approximately two ''live layers'' if a constant MOKE amplitude per atomic layer is assumed.

The desorption of hydrogen is known to occur at a temperature of about 320–330 K,[43] which coincides with the vanishing of the MOKE signal upon heating. This suggests that the vanishing of the Kerr signal at this temperature may not be assigned to an intrinsic Curie temperature of the H/Fe/Cu(001) system, but is caused by the change of the hydrogen coverage. The actual coverage at a given temperature is determined (in thermodynamical equilibrium) by the H_2 partial pressure in the UHV chamber. Therefore the MOKE signal should vanish at higher temperatures for higher hydrogen pressures. This is exactly what we observe in Fig. 3. There the polar MOKE ellipticity is shown for a 4-ML-thick Fe film upon temperature cycling, measured with a constant H_2 pressure of (a) $p_{H_2}=5\times10^{-9}$ mbar and (b) $p_{H_2}=5\times10^{-8}$ mbar and with a heating/cooling rate of 4 K/min. A small temperature hysteresis of about 10 K is observed which may be caused partially by the relatively large heating rate compared to the desorption kinetics, partly by a small temperature gradient across the sample/thermocouple. Besides that, the MOKE curves in Fig. 3(b) for the larger H_2 pressure are shifted by about 10 K with respect to the corresponding MOKE curves in Fig. 3(a) for the lower H_2 pressure. Therefore a reduction in the hydrogen coverage is responsible for the drop of the MOKE signal at temperatures around 320 K. The true Curie temperature of the (hypothetical) H-covered 4-ML film is obviously at higher temperatures. We did not go to higher hydrogen pressures and temperatures higher than 340 K because Cu segregation and pin hole formation may set in.[15]

To have an overview on the influence of hydrogen on the magnetic properties of the Fe films at various thicknesses MOKE measurements were performed on a wedgelike Fe film ranging from 2 to 5 ML. The result is shown in Fig. 4 for the clean film (a) and the film exposed to 2 L H_2 (b) for various temperatures from $T=244$ K to $T=343$ K. The curves were measured from low to high temperatures. At the lowest temperature for the clean surface some data points around 4 ML are missing because the applied magnetic field of 250 Oe was not sufficient to saturate the film. For all other cases the coercive field H_c was below 250 Oe. Let us first compare the curves for the lowest temperature: In both cases the MOKE ellipticity increases linearly with the Fe

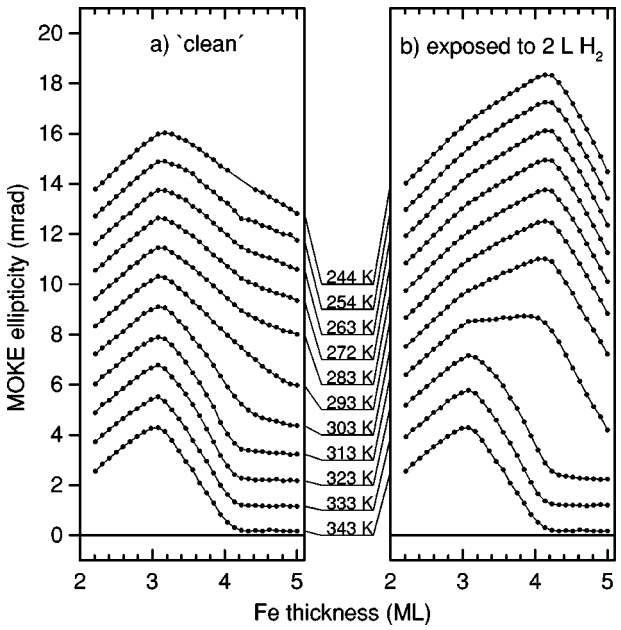

FIG. 4. Polar MOKE ellipticity vs Fe film thickness measured with an applied magnetic field of 250 Oe (a) ''clean'' and (b) H covered at 243 K for various temperatures. The curves are offset by 1 mrad with respect to each other. The line under the temperature labels indicate the zero level for that temperature. Note the curves were measured from low to high temperatures. At about 320 K hydrogen desorbs from the Fe surface.

thickness up to about 3 ML. After that the MOKE signal for the clean film decreases more or less linearly and reaches at about 5 ML that level observed in phase II corresponding to the 1.5–2 ''live layers.'' For the case of the H-covered film there is a change in slope at 3 ML but the MOKE signal increases further up to a thickness of about 4 ML before it decreases at even larger thickness. There is not much temperature dependence for a Fe thickness below 3 ML for both the clean and the H-covered film because the Curie temperature is significantly higher than the highest temperature in the plot. Also at ≈ 5 ML the temperature behavior is very similar in both cases. The Curie temperature is between 303 and 313 K. Only in the thickness range from 3 to 4 ML a different temperature dependence is observed for the clean and H_2 covered Fe film.

The transition from phase I to phase II is accompanied by a strong increase of H_c at low temperatures.[16,14] In Fig. 5 polar Kerr hysteresis curves are plotted, measured at different Fe thicknesses for the hydrogen-covered film (top row) at $T = 343$ K. The hysteresis curves in the bottom row were obtained after the hydrogen was desorbed by cycling the temperature to 343 K and back to 243 K. For the hydrogen covered films a significant increase of H_c with film thickness is observed at about 4.5 ML, close to phase transition. This onset of increased H_c is shifted towards smaller thickness for the clean films in agreement with the reduced thickness at which the transition from phase I to phase II occurs.

To compare the magnetic and structural changes IV-LEED measurements a the specularly scattered *e* beam were performed on a similar wedge as for the measurements in Fig. 4 in the beam energy range from 200–320 eV. The result is shown in Fig. 6 for Fe thicknesses from 2.1–5.1

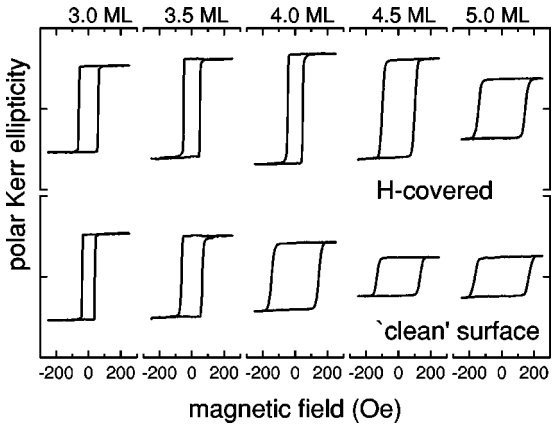

FIG. 5. Hysteresis curves of polar Kerr measurements from different positions on an Fe/Cu(001) wedge at $T = 243$ K with (top row) and without (bottom row) hydrogen coverage.

ML. The data were taken at a sample temperature of 243 K. On the left side of the figure the data for the uncovered Fe film are shown. For low thickness the characteristic double peak structure with maxima around 239 and 273 eV are clearly observable indicating the tetragonally expanded phase I. With increasing thickness the relative weight of these two peaks changes presumably because of the change from the 4×1 superstructure to the 5×1 superstructure. At about 3 – 3.5 ML, however, the 239 eV peak dies out and

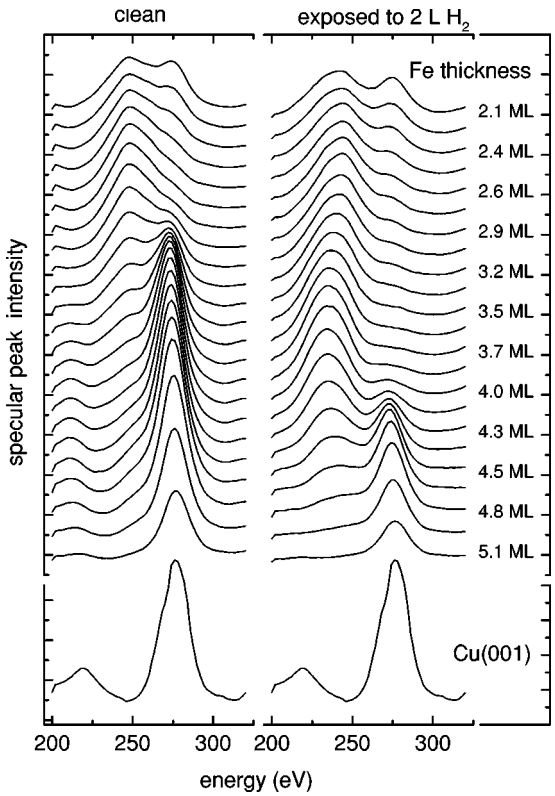

FIG. 6. IV-LEED spectra of the specularly scattered *e* beam for linearly increasing Fe thickness from 2.1 (top) to 5.1 ML (bottom) for the ''clean'' (left side) and H-covered surface (right side) at 244 K. For every second IV-LEED spectrum the thickness of the Fe film is indicated on the right. For comparison the IV-LEED spectrum from a Cu(001) surface is plotted at the bottom of the figure.

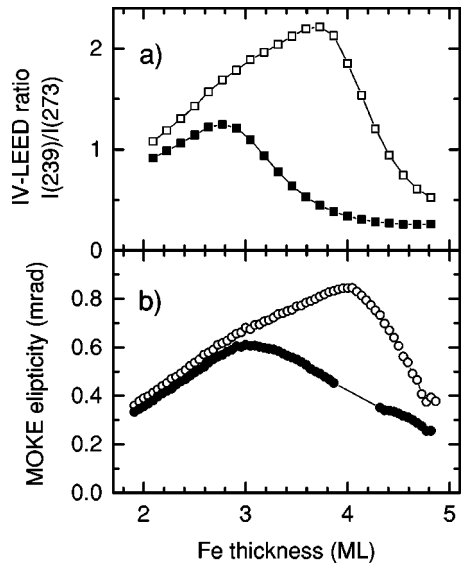

FIG. 7. Comparison (a) IV-LEED ratio I(239)/I(273) and (b) MOKE ellipticity vs Fe film thickness for the ''clean'' (solid symbols) and H-covered surface (open symbols) at 243 K.

the 273 eV peak increases in intensity. This single peak at 273 eV is the signature of the fcc phase II. Upon exposure to 2 L hydrogen at 243 K the IV-LEED spectra at low Fe thicknesses do not change much. However the 239 eV peak is visible to much larger Fe thickness and vanishes at a larger thickness of about 4.5 ML. For even larger thickness the spectra of the hydrogen covered film become very similar to those of the uncovered film. As it was shown in Ref. 13 the relative intensity of the 239 eV peak and the 273 eV peak can be used to estimate the relative fractions of phase I and II when going through the phase transition.

In Fig. 7(a) the ratio of the intensity of the peaks at 239 and 273 eV from the IV-LEED data shown in Fig. 6 is plotted versus the Fe thickness for the clean (solid symbols) and H-covered Fe film (open symbols). This ratio is compared with the MOKE ellipticity measured at the same wedge and same temperature [Fig. 7(b)]. A very similar behavior of the IV-LEED ratio and the MOKE curves is observed indicating a very close correlation of structure and magnetic properties. While below 3 ML and at about 5 ML little differences between the clean and the hydrogen covered film are observed, both in the IV-LEED peak ratio and the MOKE curves a strong difference is present in the thickness region in between. It even appears that the IV-LEED ratio exhibits the same change in slope as the MOKE measurements at 3-ML Fe thickness for the hydrogen covered case. However, the peak ratio should only be taken as a semiquantitative measure for the ratio of phase I and II. In fact, at a thickness above 3 ML the peak at 239 eV starts to shifts slightly towards lower energies, indicating a small structural change. Whether this indicates a further increase in the interlayer distance or a change in the buckling amplitude of the atoms in the layer[8] cannot be answered from the present data.

B. The effect of H_2 adsorption on the fcc-bcc transition

Figure 8 shows the polar MOKE signal from an Fe wedge on Cu(001) ranging from 0 to 12 ML at a temperature of 203 K in three different states: (a) directly after growth at 293 K and subsequent cooling down to 203 K, (b) after exposure to 3 L H_2 at 203 K, and (c) after annealing of the Fe film at 343 K for hydrogen desorption. The coercive field exceeded the maximum field of about 300 Oe in the thickness range from approximately 4 to 6 ML for the ''as-grown'' film shown in Fig. 8(a) as well as for the ''clean'' film after H exposure [Fig. 8(c)]. While the transition at 4 ML from phase I to phase II upon H_2 desorption is reversible an irreversible change is observed at the fcc-bcc transition. This transition occurs for the ''as-grown'' film at a thickness of about 10 ML indicated by the disappearance of the (remanent) polar Kerr signal. After covering the Fe wedge with hydrogen (exposure 3 L) the polar Kerr signal drops to zero already at about 8 ML and does not reappear after desorption of the hydrogen. It seems very likely that for the Fe film in the thickness range between 8 to 10 ML hydrogen adsorption has triggered the transformation of the film into the bcc phase III. Further H_2 exposure does not shift the phase II/phase III borderline to a lower thickness than 8 ML. We applied an equilibrium pressure of up to 1×10^{-7} mbar but did not see any further change in the MOKE vs thickness curve. However, an increased hydrogen pressure during the growth has a much stronger influence. This will be further

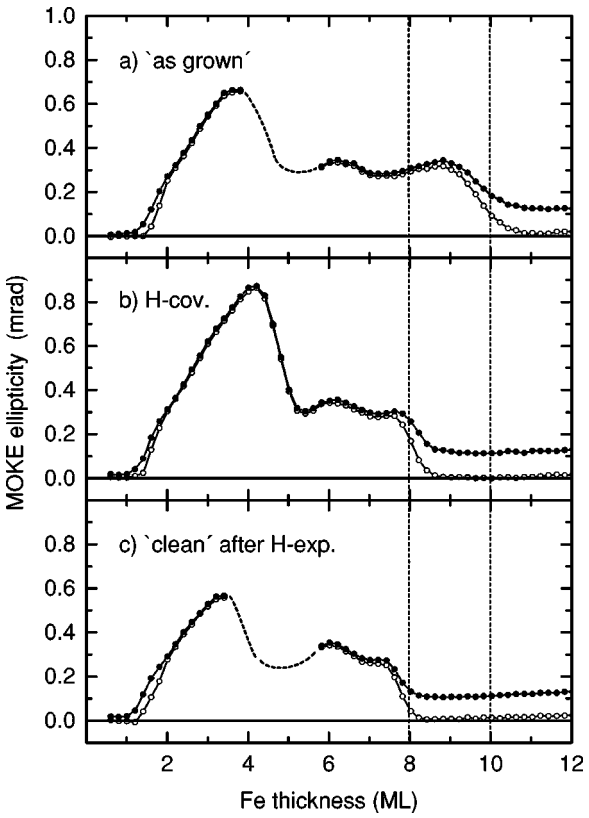

FIG. 8. Polar MOKE vs thickness from an Fe wedge measured at $T=203$ K (a) directly after growth at 293 K, (b) after exposure to 3 L of H_2 at 203 K, and (c) after annealing at 343 K. The vertical dotted lines indicate the irreversible shift of the fcc-bcc transition upon H_2 adsorption. Open and solid symbols have the same meaning as in Fig. 3. In (a) and (b) in the thickness region from 3.5 to 6 ML the coercive field exceeded the maximum external field. The dashed lines are estimates of the MOKE signal extrapolated from measurements at higher temperatures.

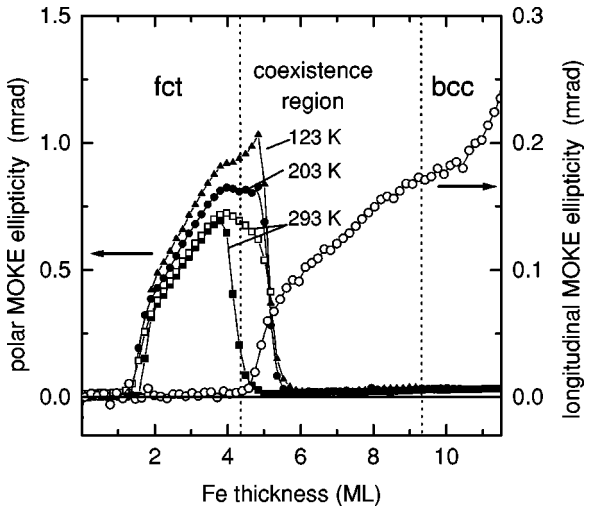

FIG. 9. Remanent polar (filled symbols, left scale) and longitudinal (open circles, right scale) MOKE vs thickness curves from an Fe wedge grown under a hydrogen atmosphere of $p_{H_2}=5\times10^{-8}$ mbar at 293 K. The vertical dotted lines separate the different structural regions as determined by the LEED. The measurements were taken at $T=203$ K (circles). For the polar MOKE, measurements taken at 123 K (triangles) and 293 K (squares) are included. The open squares indicate the polar MOKE ellipticity measurements at 293 K with an external field of about 250 Oe.

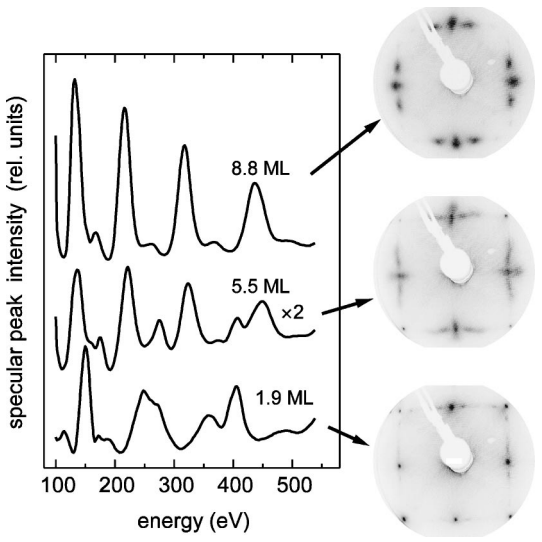

FIG. 10. IV-LEED spectra of the specularly reflected electron beam taken at an Fe thickness of 1.9, 5.5, and 8.8 ML (from bottom to top). On the left side LEED pictures of corresponding thickness for an energy of 113 eV are shown. All measurements were performed at 123 K. The angle of incidence for the IV-LEED measurements was about 6°. The intensity of the middle spectrum is multiplied by a factor of 2 with respect to the others.

corroborated by the experimental results presented in the next subsection. Note, that the Kerr signal with applied field of 250 Oe (solid symbols in Fig. 8) above 10 or 8 ML, respectively, is due to a perpendicular magnetization component and amounts roughly to the Kerr signal from half a monolayer or a tilting angle from in-plane orientation of the magnetization of about 3° for 12 ML. Because of deviation from normal incident by 6.5° the Kerr signal from the in-plane magnetization component is not zero but smaller by a factor of ≈ 50 for this geometry.

C. The influence of an enhanced H_2 pressure during the growth of the Fe film

While for all experimental results presented above the pressure inside the UHV chamber did not exceed the value of 4×10^{-10} mbar during the growth of the Fe films, in Fig. 9 the remanent polar MOKE signal vs Fe thickness is plotted for an Fe wedge grown in a hydrogen atmosphere of $p_{H_2}=8\times10^{-8}$ mbar. The growth temperature was 293 K. The solid symbols represent the remanent Kerr signal obtained in the polar geometry, while the open circles are those for the longitudinal Kerr geometry. Comparing the polar Kerr signal with that of Fig. 8(b), where the Fe surface was saturated with hydrogen (at 203 K), one sees that the region of large polar Kerr signal is even more extended up to 5 ML. However, no intermediate phase II exists anymore. The polar Kerr signal rapidly drops to zero and at the same time the longitudinal Kerr signal increases. This behavior strongly reminds one of the magnetic behavior of low-temperature-grown films.[29,30] While the temperature dependence of the remanent Kerr signal in the thickness range up to about 4 ML is only moderate for temperatures up to 293 K, in the region between 4 and 5 ML a strong temperature dependence is observed very similar to that observed in Ref. 29 for a low-temperature-grown film.[44] We note that it is only the remanent signal which disappears at 293 K. The Kerr signal with an applied field of about 250 Oe has still a value far from zero in this thickness range (open squares in Fig. 9).

To confirm that also the structural properties are similar to those known for the low-temperature-grown Fe films, LEED and IV-LEED measurements were performed on the same wedge as used for the MOKE measurements of Fig. 9. The result is displayed in Fig. 10. IV-LEED measurements of the specularly scattered electron beam are recorded on three different positions on the Fe wedge corresponding to a thickness of 1.9, 5.5, and 8.8 ML. The diffraction image (at normal incidence) at an energy of 113 eV is shown on the side for each of the three thicknesses. The IV-LEED spectrum at 1.9 ML shows the typical double peak structure known to be a signature of the tetragonally expanded fct phase I while the spectrum for the 10-ML-thick film shows single narrow peaks at positions corresponding to the interlayer spacing of bcc Fe with (110) orientation (phase III). The IV-LEED spectrum at 5.5 ML can be interpreted as a superposition of the phase I and phase III structures. The structural change can also be observed in the LEED images. The image of the 1.9-ML-thick film shows sharp spots with weak superstructure spots corresponding to the (1×5) superstructure of the fct phase.[8] In the image of the 10.2-ML-thick Fe film the so-called ''(3×1)'' superstructure, originating from four different domains of the (110) bcc phase, is clearly visible.[2] In the intermediate thickness of 5.5 ML the ''(3×1)'' superstructure peaks are washed out to streaks. This streaks indicate a reduced coherence length of the bcc structure along one of the $\langle110\rangle$ directions, while the direction perpendicular to it shows long-range order as it is expected from needlelike bcc precipitates in an fcc matrix. These precipitates have been observed even in room-temperature-grown

Fe films without intentionally increased H_2 pressure.[9,27] However, the bcc fraction in phase II remained quite low and was barely visible in the IV-LEED spectra. In our case of a room-temperature-grown Fe film under H_2 atmosphere a major part of the film is transformed into the bcc phase at 5.5 ML.

III. DISCUSSION

Hydrogen adsorption on ultrathin Fe, Co, and Ni films on Cu(001) has been investigated before by Mankey *et al.*[43] In agreement with the consideration that hydrogen transfers electrons to the transition metal it is found that for the strong ferromagnets Ni and Co hydrogen adsorption reduces the magnetization while for the weak ferromagnet Fe hydrogen enhances the magnetization slightly. However, these purely electronic effects are comparably small compared to the changes at 4 ML observed by us. In Ref. 43 the MOKE signal increased by about 20% for a 2-ML Fe film upon hydrogen coverage in qualitative agreement with our findings. Therefore we feel that the strong changes at 4 ML upon hydrogen exposure are definitely accompanied by structural changes.

Most previous investigations determined the transition thickness at about 4 ML.[7,13,16,17,21,41] However, it was already recognized by Zharnikov *et al.*[12] that the Fe films follow the expected scaling law $[T_C(\infty)-T_C(d)]\propto d^{\lambda}$, with d the film thickness and $T_C(d)$ the Curie temperature at that film thickness, only up to a thickness of 3 ML. A lower Curie temperature has been measured for the 4-ML film compared to that of the 3-ML film and therefore the authors concluded that the 4-ML film is unstable and undergoes a structural transition with a lower Curie temperature. Platow, Farle, and Baberschke[41] found by ferromagnetic resonance measurements that at 4 ML the two magnetic phases I and II coexist at low temperatures. Upon heating—which is accompanied by a change in the hydrogen coverage as we have shown above—the relative fractions of these two phases change until at about 320 K, where the hydrogen is fully desorbed, only the phase II remains. Also the strong increase of the coercivity close to the fct-fcc transition was interpreted by Berger *et al.*[14] by domain formation: The film breaks locally into regions of phase I and phase II. Because of the reduced wall energy in phase II (because of the reduced magnetization) the domain walls are trapped at these phase II patches which leads to a strongly enhanced coercive field. We have shown in this paper that the 4-ML film is stabilized by hydrogen adsorption. The 4-ML film can be reversibly switched between the two phases by hydrogen adsorption and desorption. Nevertheless, the coexistence of patches of phase I and phase II in the transition region as described in Refs. 41 and 14 seems to be correct: Our finding, that for the clean Fe film the onset of an increased coercive field is lowered by approximately 1 ML with respect to the uncovered film, supports the idea that the decay of the film into patches of phase I and phase II is delayed by hydrogen adsorption up to 4 ML. For the clean surface this probably happens already at 3 ML by the same mechanism as described above.

One may want to interpret the change in slope of the MOKE signal at 3 ML shown in Figs. 4 and 7 for the hydrogen covered Fe film by a similar mechanism. Hydrogen may not be able to fully stabilize the Fe film in phase I but a small fraction of the film at 4 ML is already transformed into phase II. However, H_c for the H-covered case increases only after 4 ML. Actually we measured the lowest H_c at about 4 ML. H_c increases rapidly for thickness larger than 4 ML. Therefore the alternative explanation of a single magnetic phase (possibly modulated in space) which changes continuously within the thickness range from 3 to 4 ML may be more likely than the formation of patches of two different magnetic phases. We note that even in the two phase region above 4 ML for the H-covered film (or 3 ML for the clean film) the magnetic patches do not coincide with the structural island size. The magnetic patches were found to be of the order 600 Å,[41] while the islands are one order of magnitude smaller.[45]

Our result that the uncovered Fe film transforms already at a thickness slightly larger than 3 ML into the magnetic phase II brings the experimental result closer to the results of theoretical calculations. While the calculations of Szunyogh, Újafalussy, and Weinberger[26] predict an antiferromagnetic spin alignment for an Fe thickness of 3 ML, Lorenz and Hafner[46] as well as Asada and Blügel[23] find a ferromagnetic ground state for 3 ML. However *all* calculations predict a partially antiferromagnetic coupling between layers at 4 ML, which is now in closer agreement with the experiment. Theoretical calculation of the H-covered fcc/fct Fe(001) film are not yet available, though highly desirable to complete the picture.

The irreversible changes at the fcc-bcc transition are of a different nature. Such an irreversible change of the structure upon hydrogen exposure at low temperatures was previously observed by Egawa, McCash, and Willis[32] for an Fe film thickness of about 10 ML. As it is now known from LEED (Ref. 2) and STM investigations,[9,27] bcc Fe precipitates are formed with (110) orientation. They can appear at a thickness down to ≈ 5 ML's but there they make only a very small fraction of the total film volume. Near 10 ML the relative weight of this bcc phase increases very rapidly and becomes the major part of the film. While the film below this transition is very flat and grows nearly in a perfect layer-by-layer growth mode the transition is accompanied by a strong reordering of the entire film resulting in a quite rough surface.

Because the bcc structure is the thermodynamically stable modification of iron at room temperature, it is not surprising that this transformation cannot be reversed upon removal of the adsorbed hydrogen. However, it is not yet clear in which way the hydrogen destabilizes the fcc phase. It was shown that the fcc phase can be stabilized beyond 10 ML by adsorption of CO during the growth.[16,47] In the detailed investigation of Ref. 47 this stabilization effect was explained by an incorporation of carbon into the film preventing the formation of bcc precipitates while oxygen acts as a surfactant and supports the layer-by-layer growth. As a major reason for the stabilization of the fcc structure the incorporation of carbon on interstitial sites was suggested, which stabilizes the fcc phase of Fe and expands the lattice and therefore reduces the natural mismatch of the (fcc) lattice constant of the Fe with respect to that of the Cu substrate lattice. This mechanism, however, cannot apply for the opposite effect of

hydrogen incorporation discussed in the present paper. Opposite to carbon, where several percent of carbon can be dissolved, the solubility of hydrogen in iron is very low. At room temperature and 1 bar H_2 pressure the atomic ratio H/Fe is below (3×10^{-8}).[48,49] This is also true for the fcc phase (γ phase), where the ratio H/Fe is below 5×10^{-4} at the melting temperature of iron. On the other hand, it is known that a very tiny amount of hydrogen (of the order of parts per million) leads to an embrittlement of iron and many other transition metals, because it is accumulated at potential fracture sites. In addition, it was shown in Ref. 50, that hydrogen dissolved in bcc iron weakens the Fe-Fe bonds of the neighboring Fe atom.[50] This effect is more pronounced for a hydrogen atom at a vacancy site compared to hydrogen adsorbed on the surface. This may reduce the activation energy necessary for the initiation of the shear process involved in the transformation of the fcc Fe film into the bcc phase. The details of this process, however, how this weakening of the Fe-Fe bonding leads to the observed destabilization of the fcc phase, is still unclear. Further investigations are necessary for clarification.

IV. CONCLUSIONS

We have shown in this paper that the tetragonally expanded phase I in Fe/Cu(001) can be stabilized by hydrogen adsorption after growth at $\approx$300 K up to 4 ML while the uncovered Fe film starts to transform slightly above 3 ML into the fcc phase II. Our observations are consistent with a coexistence region of phase I and phase II between 3 and 5 ML for the uncovered film and 4 to 5 ML for the hydrogen covered film. This switching of the 4-ML film upon hydrogen coverage is completely *reversible*. The structural and magnetic properties are strongly connected. The transition at 4-ML Fe is not driven directly by temperature but by the change of hydrogen coverage with temperature.

We observed an *irreversible* shift to thinner Fe films for the transformation of the fcc film into the bcc structure from about 10 ML down to 8 ML upon less than 3 L hydrogen exposure. Fe films up to 8 ML are stable even under a hydrogen equilibrium pressure of up to at least 1×10^{-7} mbar. However, Fe films grown at room temperature ($\approx$300 K) in an H_2 atmosphere of 5×10^{-8} mbar show a structural and magnetic behavior as it was reported for low-temperature-grown ($\approx$100 K) Fe films. We suggest that the (almost unavoidable) hydrogen coverage of low-temperature-grown Fe films may be (at least partly) responsible for the observed structural and magnetic differences to the room-temperature-grown films. Our findings underline the potential influence of hydrogen absorption on the magnetic and structural properties of epitaxial metallic layers

[1] J. Thomassen, B. Feldmann, and M. Wuttig, Surf. Sci. **264**, 406 (1992).
[2] M. Wuttig, B. Feldmann, J. Thomassen, F. May, H. Zillgen, A. Brodde, H. Hannemann, and H. Neddermeyer, Surf. Sci. **291**, 14 (1993).
[3] P. Bayer, S. Müller, P. Schmailzl, and K. Heinz, Phys. Rev. B **48**, 17 611 (1993).
[4] Th. Detzel, N. Memmel, and Th. Fauster, Surf. Sci. **293**, 227 (1993).
[5] K.E. Johnson, D.D. Chambliss, R.J.W. Wilson, and S. Chiang, J. Vac. Sci. Technol. A **11**, 1654 (1993).
[6] A. Fuest, R.D. Ellerbrock, A. Schatz, W. Keune, R.A. Brand, and H.-D. Pfannes, Hyperfine Interact. **92**, 1297 (1994).
[7] S. Müller, P. Bayer, C. Reischl, K. Heinz, B. Feldmann, H. Zillgen, and M. Wuttig, Phys. Rev. Lett. **74**, 765 (1995).
[8] S. Müller, P. Bayer, A. Kinne, P. Schmailzl, and K. Heinz, Surf. Sci. **322**, 21 (1995).
[9] J. Giergiel, J. Shen, J. Woltersdorf, A. Kirilyuk, and J. Kirschner, Phys. Rev. B **52**, 8528 (1995).
[10] M. Wuttig, B. Feldmann, and T. Flores, Surf. Sci. **331-333**, 659 (1995).
[11] Th. Detzel, M. Vonbank, M. Donath, N. Memmel, and V. Dose, J. Magn. Magn. Mater. **152**, 287 (1996).
[12] M. Zharnikov, A. Dittschar, W. Kuch, C.M. Schneider, and J. Kirschner, Phys. Rev. Lett. **76**, 4620 (1996).
[13] M. Zharnikov, A. Dittschar, W. Kuch, C.M. Schneider, and J. Kirschner, J. Magn. Magn. Mater. **174**, 40 (1997).
[14] A. Berger, B. Feldmann, H. Zillgen, and M. Wuttig, J. Magn. Magn. Mater. **183**, 35 (1998).
[15] J. Shen, C. Mohan, P. Ohresser, M. Klaua, and J. Kirschner, Phys. Rev. B **57**, 13 674 (1998).
[16] J. Thomassen, F. May, M. Wuttig, and H. Ibach, Phys. Rev. Lett. **69**, 3831 (1992).
[17] D. Li, M. Freitag, J. Person, Z.Q. Qiu, and S.D. Bader, Phys. Rev. Lett. **72**, 3112 (1994).
[18] Th. Detzel, M. Vonbank, M. Donath, and V. Dose, J. Magn. Magn. Mater. **147**, L1 (1995).
[19] R.D. Ellerbrock, A. Fuest, A. Schatz, W. Keune, and R.A. Brand, Phys. Rev. Lett. **61**, 475 (1995).
[20] W. Keune, A. Schatz, R.D. Ellerbrock, A. Fuest, K. Wilmers, and R.A. Brand, J. Appl. Phys. **79**, 4265 (1996).
[21] M. Straub, R. Vollmer, and J. Kirschner, Phys. Rev. Lett. **77**, 743 (1996).
[22] B. Újfalussy, L. Szunyogh, and P. Weinberger, Phys. Rev. B **54**, 9883 (1996).
[23] T. Asada and S. Blügel, Phys. Rev. Lett. **79**, 507 (1997).
[24] T. Kraft, P.M. Marcus, and M. Scheffler, Phys. Rev. B **49**, 11 511 (1994).
[25] R. Lorenz and J. Hafner, J. Magn. Magn. Mater. **157/158**, 514 (1996).
[26] L. Syunyogh, B. Újafalussy, and P. Weinberger, Phys. Rev. B **55**, 14 392 (1997).
[27] J. Giergiel, J. Kirschner, J. Landgraf, J. Shen, and J. Woltersdorf, Surf. Sci. **310**, 1 (1994).
[28] D. Pescia, M. Stampanoni, G.L. Bona, A. Vaterlaus, R.F. Willis, and F. Meier, Phys. Rev. Lett. **58**, 2126 (1987).
[29] D.P. Pappas, K.-P. Kämper, and H. Hopster, Phys. Rev. Lett. **64**, 3179 (1990).
[30] R. Allenspach and A. Bishof, Phys. Rev. Lett. **69**, 3385 (1992).
[31] H. Landskron, G. Schmidt, K. Heinz, K. Müller, C. Stuhlmann, U. Beckers, M. Wuttig, and H. Ibach, Surf. Sci. **256**, 115 (1991).
[32] C. Egawa, E.M. McCash, and R.F. Willis, Surf. Sci. **215**, L271 (1989).

[33] H. Zillgen, B. Feldmann, and M. Wuttig, Surf. Sci. **321**, 32 (1994).
[34] R. Vollmer, S. van Dijken, M. Schleberger, and J. Kirschner Phys. Rev. B **61**, 1303 (2000).
[35] J. Giergiel, H. Hopster, J.M. Lawrence, J.C. Hemminger, and J. Kirschner, Rev. Sci. Instrum. **66**, 3475 (1995).
[36] M. Zharnikov, A. Dittschar, W. Kuch, K. Meinel, C.M. Schneider, and J. Kirschner, Thin Solid Films **275**, 262 (1996).
[37] A. Braun, B. Feldmann, and M. Wuttig, J. Magn. Magn. Mater. **171**, 16 (1997).
[38] J. Shen, M. Klaua, P. Ohresser, H. Jenniches, J. Barthel, C.V. Mohan, and J. Kirschner, Phys. Rev. B **56**, 11 134 (1997).
[39] H. Jenniches, J. Shen, C.V. Mohan, S.S. Manoharan, J. Barthel, P. Ohresser, M. Klaua, and J. Kirschner, Phys. Rev. B **59**, 1196 (1999).
[40] J. Shen, P. Ohresser, C.V. Mohan, M. Klaua, J. Barthel, and J. Kirschner, Phys. Rev. Lett. **80**, 1980 (1998).
[41] W. Platow, M. Farle, and K. Baberschke, Europhys. Lett. **43**, 713 (1998).
[42] P. Poulopoulos, M. Farle, U. Bovensiepen, and K. Baberschke, J. Magn. Magn. Mater. **177-181**, 1225 (1998).
[43] G.J. Mankey, M.T. Kief, F. Huang, and R.F. Willis, J. Vac. Sci. Technol. A **11**, 2034 (1993).
[44] Note that in Ref. 29 the thickness calibration bases on ''kinks'' in the Auger intensity curve vs film thickness is probably in error by a factor of 2. As shown in Ref. 31 the occurrence of superstuctures may be responsible for the introduction of kinks in the Auger intensity curve rather than the completion of a monolayer.
[45] J. Shen, J. Giergiel, A.K. Schmid, and J. Kirschner, Surf. Sci. **328**, 32 (1995).
[46] R. Lorenz and J. Hafner, Phys. Rev. B **54**, 15 937 (1996).
[47] A. Kirilyuk, J. Giergiel, M. Straub, and J. Kirschner, Phys. Rev. B **54**, 1050 (1996).
[48] R.G. da Silva and R.B. McLellan, J. Less-Common Met. **50**, 1 (1976).
[49] A. San-Martin and F. D. Manchester, *Binary Alloy Phase Diagrams*, edited by Th. B. Massalski (ASM International, Materials Park, OH, 1990), Vol. 2.
[50] A. Juan and R. Hoffmann, Surf. Sci. **421**, 1 (1999).